Molecular Crystals and Liquid Crystals

Publication details, including instructions for authors and subscription information:
http://www.tandfonline.com/loi/gmcl20

Modelling Polarization Effects in a Freely Suspended Smectic Liquid Crystal Film

H. Millar [a] & G. McKay [a]

[a] Department of Mathematics, University of Strathclyde, Glasgow, Scotland, United Kingdom

Version of record first published: 22 Sep 2010

To cite this article: H. Millar & G. McKay (2007): Modelling Polarization Effects in a Freely Suspended Smectic Liquid Crystal Film, Molecular Crystals and Liquid Crystals, 478:1, 45/[801]-55/[811]

To link to this article: http://dx.doi.org/10.1080/15421400701732027

Mol. Cryst. Liq. Cryst., Vol. 478, pp. 45/[801]–55/[811], 2007

ISSN: 1542-1406 print/1563-5287 online
DOI: 10.1080/15421400701732027

Taylor & Francis
Taylor & Francis Group

Modelling Polarization Effects in a Freely Suspended Smectic Liquid Crystal Film

H. Millar
G. McKay
Department of Mathematics, University of Strathclyde, Glasgow, Scotland, United Kingdom

We consider a smectic liquid crystal film freely suspended between two electrodes and subject to an electric field. For a fixed voltage the system can exhibit qualitatively different types of equilibrium director profile, depending on the spontaneous polarization and flexoelectric contributions to the bulk free energy. We examine the stability of the calculated director profiles and determine which configurations are energetically favourable. Furthermore, we also observe that, at critical values of the polarization parameters, there exists a bifurcation corresponding to a change in the number of equilibrium profiles. Generally, any configuration where the electric field and spontaneous polarization act in opposing directions is energetically unfavourable. However, we show that these profiles can become metastable and local energy minima when the flexoelectric parameters are relatively large.

Keywords: continuum theory; polarization; smectic liquid crystals

INTRODUCTION

We examine the static director configurations of a smectic liquid crystal film freely suspended between two electrodes. The film is subject to an electric field applied in a direction parallel to both the layers and the two free surfaces (see, for example, Schlauf *et al*. [1]). If the temperature of the liquid crystal is reduced towards the SmA^* – SmC^* phase transition, the layers at the surface transform into the low-temperature SmC^* phase well above the bulk transition [2,3].

Extending the model of McKay *et al*. [4], we examine the competing effects of flexoelectricity and spontaneous polarization on the smectic film.

Address correspondence to G. McKay, Department of Mathematics, University of Strathclyde, 26 Richmond Street, Glasgow, G1 1XH, Scotland, United Kingdom. E-mail: gmck@maths.strath.ac.uk

This modelling is based upon a continuum theory for smectics that allows variation in the smectic layer spacing and the molecular tilt. The temperature of the sample is fixed above the SmA* – SmC* phase transition temperature, therefore the bulk of the film is homeotropically aligned. However, we incorporate the SmC* ordering at the surface via weak anchoring of the molecular tilt. We calculate equilibrium director configurations by minimizing the total free energy of the liquid crystal per unit area. This total free energy incorporates elastic, spontaneous polarization and flexoelectric effects as well as the surface energy due to the weak anchoring. We will show that the liquid crystal exhibits different types of director twist profile depending on the relative sizes of the polarization coefficients. In particular, the presence of a flexoelectric polarization can stabilize an otherwise unstable configuration.

MODEL

We consider a SmA* liquid crystal film suspended between two electrodes. The smectic layers are assumed to lie parallel to the free surfaces at $z = 0$ and $z = h$, where h is the depth of the film (see Fig. 1). We represent the liquid crystal director via a unit vector

$$\underline{n} = (\sin\theta\cos\phi, \sin\theta\sin\phi, \cos\theta).$$

The director tilt angle $\theta(z)$ and polar twist angle $\phi(z)$ are functions of the cell height only as we assume that within each smectic layer the directors are parallel. The projection of the director $\underline{n}$ onto the smectic layer is the vector $\underline{c} = \sin\theta(\cos\phi, \sin\phi, 0)$.

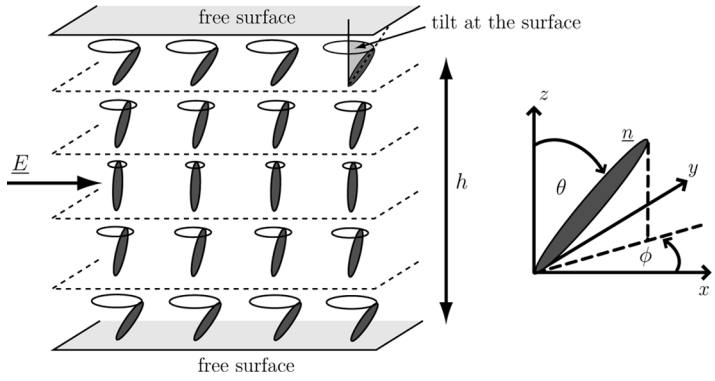

FIGURE 1 Schematic of the liquid crystal film illustrating twist out of the vertical plane due to polarization.

The in-plane electric field may be represented via

$$\underline{E} = \frac{V}{d}(1, 0, 0),$$

where V is the applied voltage and d is the width of the film layer. An effective polarization, $\underline{P}$, is introduced as the sum of a spontaneous polarization term, $\underline{P}_{sp}$, and $\underline{P}_{fl}$, the contribution due to flexoelectricity. We adopt a spontaneous polarization from the work of Osipov and Pilkin [5],

$$\underline{P}_{sp} = P_s(\underline{n} \cdot \hat{\underline{a}})\underline{n} \times \hat{\underline{a}} = P_s \cos\theta \sin\theta(\sin\phi, -\cos\phi, 0), \quad (1)$$

where $\hat{\underline{a}} = (0, 0, 1)$ is a unit vector normal to the smectic layers and P_s is the magnitude of the spontaneous polarization. The flexoelectric polarization may be written using a 'tilted uniaxial' description [6] as

$$\underline{P}_{fl} = e_{11}\ \underline{n}(\nabla \cdot \underline{n}) + e_{33}(\nabla \times \underline{n}) \times \underline{n} + \beta_1\ \underline{n}(\underline{n} \cdot \nabla\gamma) + \beta_3(\nabla\gamma - \underline{nn} \cdot \nabla\gamma), \quad (2)$$

where e_{11} and e_{33} are contributions similar to those found in the study of nematics. The term γ is introduced to represent the interlayer spacing, which may be regarded as $\cos\theta(z)$ in this model. Any contributions arising from layer dilation parallel to the director are represented via β_1, whereas contributions perpendicular to the director correspond to the β_3 term.

ANALYSIS

We employ a bulk free energy density, w_b, similar to Nakagawa [7] (and employed elsewhere, e.g., McKay *et al*. [4]),

$$2w_b = K(|\underline{c}|^2 - \sin^2\theta_0)^2 + A(\nabla \cdot \underline{a})^2 + C\ \mathrm{tr}(\nabla\underline{c}\nabla\underline{c}^T) - 2\underline{P} \cdot \underline{E}, \quad (3)$$

where K, A and C are all non-negative elastic constants. The dilation term $K(|\underline{c}|^2 - \sin^2\theta_0)^2$ is a measure of the energy cost as the molecular tilt angle deviates from θ_0, the expected fixed director tilt angle in the absence of boundary or electric field effects. As we are studying a SmA* sample at a fixed temperature above the SmA* – SmC* phase transition, we set $\theta_0 = 0^\circ$.

To model the expected SmC* behaviour at the surfaces $z = 0$ and $z = h$ we introduce a surface energy density, w_s, adapted from the work of Rapini and Papoular [8],

$$w_s = w_0 \sin^2(\theta - \theta_w), \quad (4)$$

where ω_0 is the strength of the anchoring and θ_w is a prescribed pretilt angle at the free surfaces. The surface energy can achieve its absolute

minimum if $\theta = \theta_w$, i.e. if the director tilt at the surface coincides with the angle θ_w. Due to the competition between the various components of w_b in (3), in particular the dilation term measuring the deviation from $\theta_0 = 0^\circ$ in the bulk, the actual tilt exhibited at the free surfaces may differ from θ_w.

We can now calculate W, the total free energy of our sample, as

$$W = \int_{\mathcal{V}} w_b \, d\mathcal{V} + \int_{\mathcal{S}} w_s \, d\mathcal{S}. \tag{5}$$

Here $\mathcal{V}$ is the volume of our sample and $\mathcal{S}$ represents the surfaces $z = 0$ and $z = h$. Equilibrium equations for the bulk of the film are derived by minimizing the free energy W. The corresponding Euler-Lagrange equations are

$$\left(\frac{\sin\theta}{\cos^2\theta} + F^2\frac{\cos^4\theta}{\sin\theta}\right)\theta'' + \left(\frac{1+\sin^2\theta}{\cos^3\theta} - F^2\cos^3\theta\right)(\theta')^2 - D^2\cos^3\theta\sin^2\theta - F^2(\phi')^2\cos^3\theta + \widehat{P_s}\frac{\cos 2\theta\cos^2\theta}{\sin\theta}\sin\phi - \widehat{P}_{f_1}\phi'(1+\mu\cos\theta)\sin\theta\cos^2\theta\sin\phi = 0, \tag{6}$$

$$\phi'' + \frac{2}{\tan\theta}\theta'\phi' + \frac{\widehat{P_s}}{F^2}\frac{\cos\phi}{\tan\theta} + \frac{\widehat{P}_{f_1}}{F^2}\theta'(1+\mu\cos\theta)\sin\phi = 0. \tag{7}$$

These equations have been non-dimensionalized by introducing $\hat{z} = z/h$ and are valid for the region $0 < \hat{z} < 1$. The prime $'$ denotes differentiation with respect to the rescaled variable $\hat{z}$, while angles θ and ϕ are now functions of $\hat{z}$. Dimensionless parameters have been introduced via

$$D^2 = \frac{Kh^2}{2\pi^2 A}, \quad F^2 = \frac{C}{4\pi^2 A}, \quad \widehat{P_s} = \frac{P_s V h^2}{4\pi^2 A d},$$
$$\widehat{P}_{f_1} = \frac{Vh(e_{11}-e_{33})}{4\pi^2 A d}, \quad \mu = \frac{\beta_1 - \beta_3}{e_{11}-e_{33}}.$$

Parameter D^2 is a measure of the elastic energy associated with compression or dilation of individual smectic layers, while F^2 is the elastic contribution due to molecular twist across the cell. The Goldstone mode [9] dictates that compression or dilation of smectic layers is more difficult than twist, therefore we expect $D^2 \gg F^2$. Parameters $\widehat{P_s}$ and $\widehat{P}_{f_1}$ measure the spontaneous and flexoelectric contributions, respectively, relative to the elastic constant A. Parameter μ is a ratio of the contributions arising from the flexoelectric coefficients.

We formulate weak boundary conditions for the tilt and "natural" conditions for the twist at $\hat{z} = 0$ or $\hat{z} = 1$ via a balance of couples relating the bulk energy w_b and surface energy w_s [10]:

$$\left(\frac{\tan^2\theta}{\cos^2\theta} + F^2\cos^2\theta\right)\theta' + \widehat{P}_{f_2}\left(\frac{e_{11}}{e_{33}}\sin^2\theta - \cos^2\theta\right)\cos\phi = \mp\frac{h}{4\pi^2 A}\omega_0 \sin 2(\theta - \theta_w), \tag{8}$$

$$\phi' + \frac{\widehat{P}_{f_2}}{F^2}\frac{\sin\phi}{\tan\theta} = 0. \tag{9}$$

The $-$ and $+$ signs on the right hand side of (8) correspond to conditions at $\hat{z} = 0$ and $\hat{z} = 1$, respectively, whereas (9) is appropriate at both surfaces. We have also introduced $\widehat{P}_{f_2} = Vhe_{33}/(4\pi^2 Ad)$, a dimensionless flexoelectric coefficient which manifests itself only in the surface conditions.

EQUILIBRIUM PROFILES

In order to derive equilibrium director tilt and twist profiles for our smectic film, we require to solve Eqs. (6) and (7) subject to boundary conditions (8), (9). This has been carried out numerically and, unless otherwise stated, in our subsequent discussions the following parameter values have been chosen:

$$A = 10^{-11}\text{N}, \quad C = 5\times 10^{-12}\text{N}, \quad K = 500\,\text{Nm}^{-2}, \quad h = 2\times 10^{-6}\,\text{m},$$
$$d = 10^{-3}\text{m}, \quad e_{11} = 2\times 10^{-11}\,\text{Cm}^{-1}, \quad e_{33} = 10^{-11}\,\text{Cm}^{-1},$$
$$V = 10\,\text{V}, \quad \omega_0 = 1\,\text{Nm}^{-1}, \quad \theta_w = 20^\circ.$$

Additionally, the ratio of flexoelectric coefficients μ is set to zero as we have set $\beta_1 = \beta_3$. Due to the trigonometric terms, system (6)–(9) is periodic in the twist angle ϕ. Each set of solutions for the twist profile will re-occur with period 360°. However, in the following we concentrate on one family of solutions close to $\phi = 0^\circ$.

Figure 2 demonstrates that, for the given set of parameter values and a relatively small spontaneous polarization coefficient $P_s = 10^{-8}\,\text{Cm}^{-2}$, we obtain four straightforward and distinct director twist solutions. However, the tilt profiles corresponding to the four twist solutions are virtually indistinguishable from one another. The anchoring strength, ω_0, chosen corresponds to a strong anchoring condition, therefore in Fig. 2(a) at either surface there is little deviation

from the pretilt angle $\theta_w = 20°$. Due to the competing effects of SmC* ordering at the surface of the film at a temperature above the SmA* – SmC* transition, the tilt in the bulk of the film is much smaller than the surface tilt.

In the following analysis we identify each type of twist solution via the value $\phi_m = \phi(1/2)$, the twist angle in the center of the film (or, by symmetry, the average twist across the sample). The four profiles in Fig. 2(b) can be characterized as, from top to bottom, $\phi_m = 90°$, $\phi_m \approx 0°$, $\phi_m = -90°$ and $\phi_m \approx -180°$ solutions, respectively. The equality in the $\phi_m = \pm 90°$ cases follows automatically from Eq. (7) and the observation that, by symmetry, $\theta'(1/2) = 0$. The opposing gradients in the twist solutions with $\phi_m = \pm 90°$ are a consequence of boundary condition (9), noting that for our chosen parameter values the ratio $\widehat{P}_{f_2}/F^2$ is positive. The twist profiles with $\phi_m \approx 0°$ and

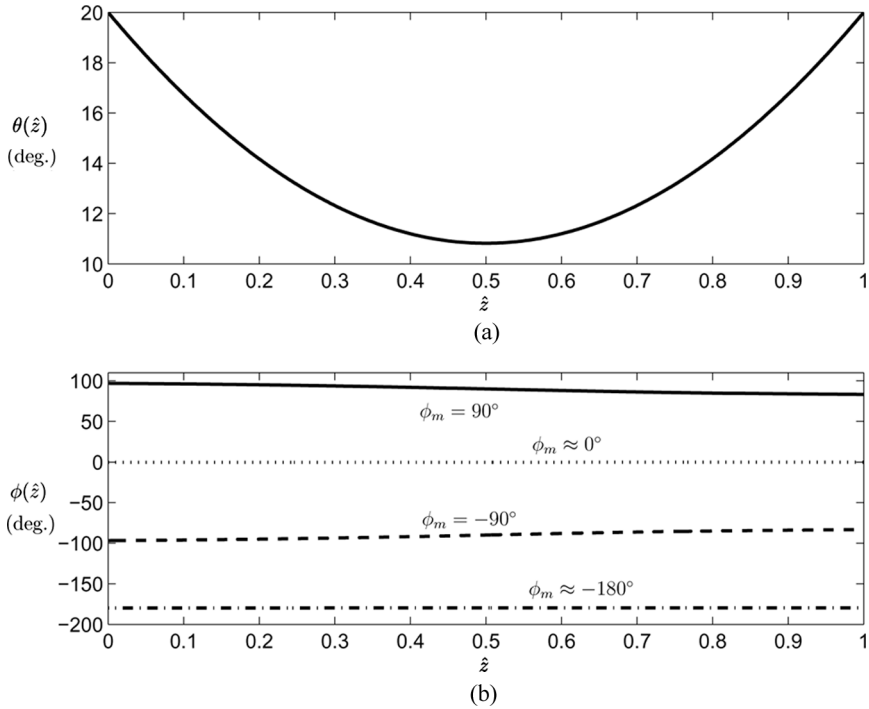

FIGURE 2 Equilibrium director profiles, (a) tilt θ (b) twist ϕ, obtained when $P_s = 10^{-8}\,\mathrm{Cm}^{-2}$. Four distinct twist profiles are present for the chosen parameter values. Note, in (a) the tilt profiles corresponding to the four distinct twist solutions are very similar and indistinguishable.

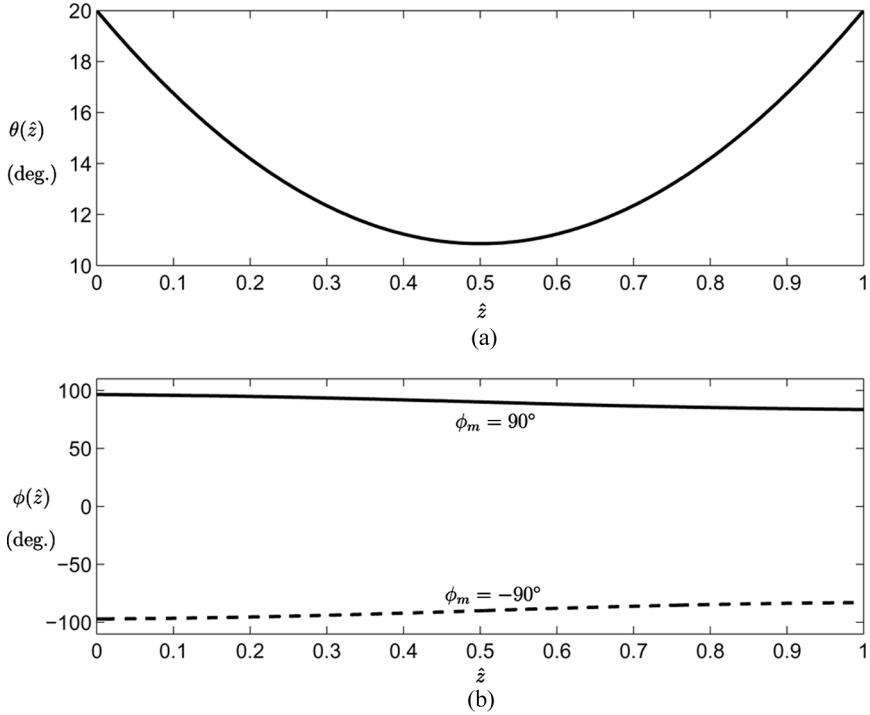

FIGURE 3 Equilibrium director profiles, (a) tilt θ (b) twist ϕ, obtained when $P_s = 10^{-5}\,\mathrm{Cm}^{-2}$. Only two twist profiles are present for the chosen parameters. In (a) the tilt profiles corresponding to the two distinct twist profiles are indistinguishable.

$\phi_m \approx -180^\circ$ exhibit gradients smaller in magnitude than the other two cases, with very little net twist across the layer.

In contrast, if we now choose a relatively large spontaneous polarization strength of $P_s = 10^{-5}\mathrm{Cm}^{-2}$, we find only two director twist profiles, as illustrated in Fig. 3. Adopting the same notation as Fig. 2, the two twist profiles may be characterized as $\phi_m = \pm 90^\circ$ and they can be associated with the extrema of the spontaneous polarization contribution to the free energy density, $-\underline{P}_{sp} \cdot \underline{E}$. Once again, the corresponding director tilt solutions for the two cases are very similar to each other.

VARIABLE SPONTANEOUS POLARIZATION

When flexoelectricity is absent from our system, or when the flexoelectric coefficients are relatively small, the spontaneous polarization

term can dominate the effective polarization $\underline{P}$ and the bulk free energy density. However, the behaviour of the system changes significantly as the influence of flexoelectricity increases (or as the spontaneous polarization coefficient decreases). We now investigate this transition from relatively small to large spontaneous polarization parameter and the associated change in the behaviour of the system (6)–(9). In order to achieve this we introduce a variable control parameter $\lambda \equiv -\log(P_s)$. As the spontaneous polarization coefficient increases, λ decreases (and vice versa).

For the parameters considered here, it is possible to obtain $\phi_m = \pm 90^\circ$ type twist solutions for all values of P_s (or λ). In Fig. 4 we concentrate on the two types of twist profile that occur only when the influence of flexoelectricity is significantly large. These correspond to the $\phi_m \approx 0^\circ$ and -180° solutions in Fig. 2(b). As the magnitude of the spontaneous polarization increases (or as λ decreases) we see that the $\phi_m \approx 0^\circ$ type solution in Fig. 2(b) (which corresponds to $\lambda = 8$) decreases towards a solution with $\phi_m = -90^\circ$. The twist solution corresponding to $\phi_m \approx -180^\circ$ converges towards a similar profile. Below a critical value of $\lambda \approx 5.79$, when the influence of flexoelectricity is relatively small, it is no longer possible to obtain twist solutions to system

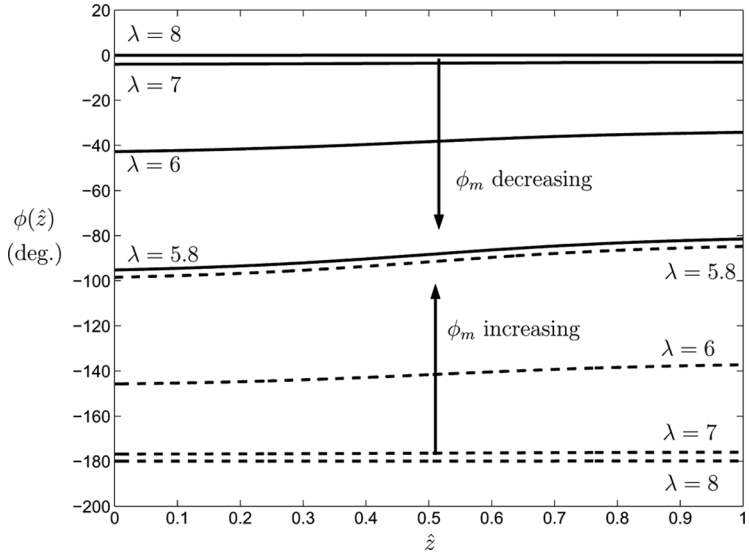

FIGURE 4 Behaviour of twist profiles when λ is large. The $\phi_m \approx 0^\circ$ (top) and $\phi_m \approx -180^\circ$ solutions (bottom, dashed) are equivalent to those in Fig. 2(b). As λ decreases, the solutions converge towards a profile with $\phi_m \approx -90^\circ$.

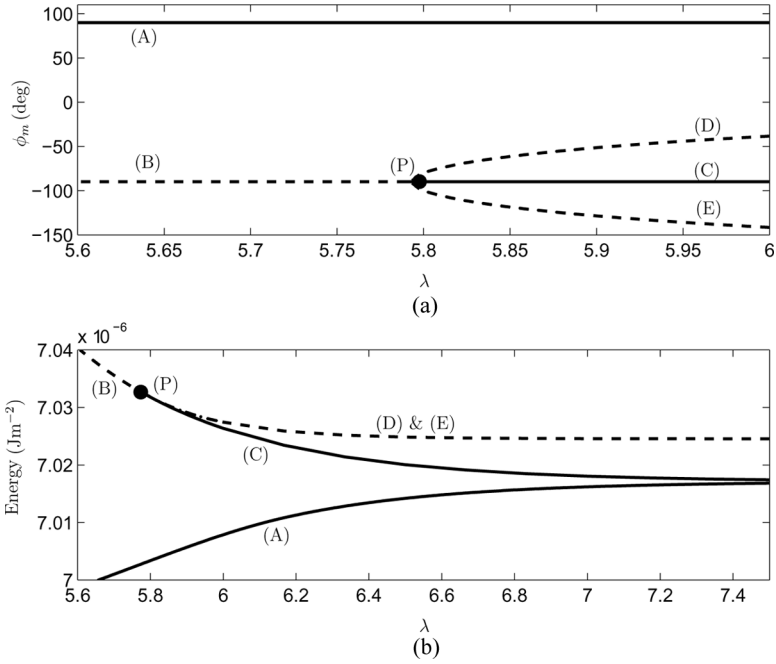

FIGURE 5 (a) Bifurcation diagram illustrating the average value of each twist profile ϕ_m as λ varies. (b) Energy per unit area as λ is varied.

(6)–(9) other than those with $\phi_m = \pm 90^\circ$. The bifurcation diagram in Fig. 5(a) illustrates this behaviour. The average of the molecular twist across the layer, ϕ_m, has been chosen as the principal solution measure and the resulting bifurcation diagram is a plot of this measure against our control parameter λ. The profiles with $\phi_m = 90^\circ$ form branch (A) and remain independent of any other profiles. However, as the magnitude of λ increases a bifurcation point (P) is found on the $\phi_m = -90^\circ$ branch (B). From this bifurcation point a pitchfork bifurcation is formed consisting of branch (C), and two parabolic branches (D) and (E).

The bifurcation diagram in Fig. 5(a) also indicates the stability of our solutions over the given parameter range. (Details of these stability calculations have been omitted.) A solid line denotes solutions that are stable to arbitrary perturbations, while a dashed line represents solutions that are unstable to perturbations. Branch (A) with $\phi_m = 90^\circ$ remains stable for all λ. However, the solutions corresponding to $\phi_m = -90^\circ$ change stability as they pass through the bifurcation point (P). In a perturbation analysis, solutions on the

unstable parabolic branches (D) and (E) are attracted to either the metastable branch (C) or branch (A). The behaviour of branches (B)–(E) is typical of a subcritical pitchfork bifurcation [11].

Further information can be derived from the total free energy per unit area in the *xy*-plane. (The free energy per unit area is defined as the sum of the integral of the energy density w_b across the thickness of the film and the energy w_s evaluated at both free surfaces.) As λ increases in Fig. 5(b) the free energies corresponding to twist solutions with $\phi_m = \pm 90^\circ$ converge, however branch (A) remains consistently lower. This is expected because a twist solution with $\phi = 90^\circ$ is a minimizer of the energy associated with the spontaneous polarization (for a positive voltage) and corresponds to the polarization $\underline{P}_{sp}$ aligning with the electric field. The case $\phi = -90^\circ$ is a maximizer corresponding to opposing $\underline{P}_{sp}$ and $\underline{E}$ fields. Beyond the bifurcation point, the energies of the unstable branches (D) and (E) are equal but are higher than the stable branches (A) and (C).

The behaviour outlined above is not unique to the chosen parameter values. In the absence of any flexoelectric contributions, i.e. $e_{11} = e_{33} = 0$, stable profiles with $\phi_m = 90^\circ$ and unstable solutions with $\phi_m = -90^\circ$ coexist. However, it is the introduction of the non-trivial flexoelectric polarization that induces a bifurcation point and stabilizes the $\phi_m = -90^\circ$ profiles. Maintaining the ratio $e_{11}/e_{33} = 2$, Fig. 6 demonstrates the relationship between the flexoelectric coefficient e_{33} and the spontaneous polarization exponent λ at the bifurcation point. Again, the region where four twist profiles can

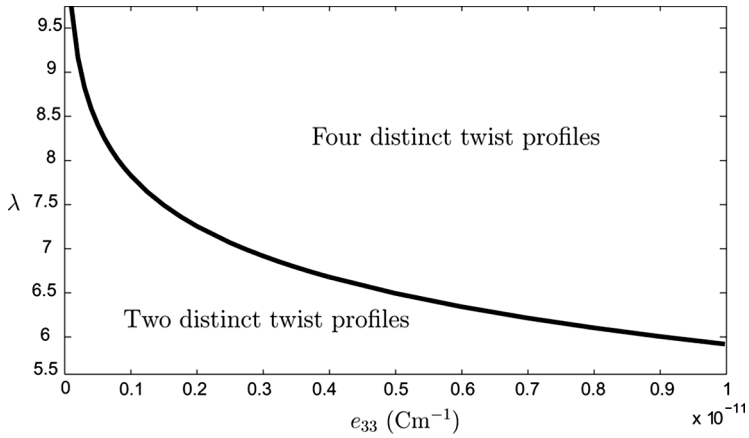

FIGURE 6 Relationship between the spontaneous polarization exponent, λ, and the flexoelectric contribution, e_{33}, at the bifurcation point.

coexist corresponds to the regime with large λ (or small P_s) and large flexoelectric coefficient e_{33}.

CONCLUSIONS

We have obtained qualitatively different types of equilibrium twist profile for a freely suspended smectic film subject to a constant electric field. When the influence of flexoelectricity was small, we found two distinct types of equilibrium twist solution, one stable and the other unstable. The stable profile corresponds to the energetically favourable alignment of the spontaneous polarization with the electric field, whilst the unstable profile is of a higher free energy and equivalent to the polarization opposing the field direction. For relatively large flexoelectric coefficients four distinct twist solutions can coexist. The presence of the two new solutions acts to stabilize the previously unstable branch. Therefore, in this regime it is possible to find two stable equilibrium configurations that are local minima of the total free energy but are very different in nature.

REFERENCES

[1] Schlauf, D., Bahr, Ch., Dolganov, V. K., & Goodby, J. W. (1999). *Eur. Phys. J. B.*, *9*, 461.
[2] Bahr, Ch. (1994). *Int. J. Mod. Phys. B*, *8*, 3051.
[3] Stoebe, T. & Huang, C. C. (1995). *Int. J. Mod. Phys. B*, *9*, 2285.
[4] McKay, G., MacKenzie, K. R., & Mottram, N. J. (2004). *Ferroelectrics*, *309*, 35–42.
[5] Osipov, M. A. & Pilkin, S. A. (1995). *J. Phys. II France*, *5*, 1223–1240.
[6] De Gennes, P. G. & Prost, J. (1993). *The Physics of Liquid Crystals*, 2nd Edition, Claredon Press: Oxford.
[7] Nakagawa, M. (1990). *Liq Cryst.*, *8*, 651–657.
[8] Rapini, A. & Papoular, M. (1969). *J. de Physique Colloq.*, *30*, 54–56.
[9] Pandey, M. B., Dhar, R., Agrawal, V. K., Dabrowski, R., & Tykarska, M. (1994). *Liq. Cryst.*, *31*, 973–987.
[10] Jenkins, J. T. & Barratt, P. J. (1974). *Q. J. Mech. Appl. Math. 27*, 111–127.
[11] Strogratz, S. H. (1994). *Nonlinear Dynamics and Chaos*, Addison-Wesley Publishing.